Electronic Supplementary Material (ESI) for Materials Horizons.

Supporting Information

Low hysteresis, water retention, anti-freeze multifunctional hydrogel strain sensor for human-machine interfacing and real-time sign language translation.

Lijuan Zhou[a], Bin Zhao[b], Jingye Liang[a], Fangying Lu[a], Weiping Yang[a], Jishuai Xu[a], Jingxuan Zheng[a], Yong Liu*[a], Run Wang*[a], Zunfeng Liu[c]

[a] School of Textile Science and Engineering, Tiangong University, 399 West Binshui Road, Tianjin 300387, China.

Email: liuyong@tiangong.edu.cn; wangrun@tiangong.edu.cn

[b] School of Artificial Intelligence, Guangxi Colleges and Universities Key Laboratory of AI Algorithm Engineering, Guilin University of Electronic Technology, Guilin Guangxi, 541004, China.

[c] State Key Laboratory of Medicinal Chemical Biology, Key Laboratory of Functional Polymer Materials, College of Chemistry Frontiers Science Center for New Organic Matter, Nankai University, 94 Weijin Road, Tianjin 300071, China.

Experimental Section

Materials

All chemical reagents were used as received. Acrylamide (Am), acrylic acid (AA), vinyltriethoxysilane (VTES), 2-hydroxy-4-(2hydroxyethyl)-2-methylpropiophenone (I2959), and calcium chloride ($CaCl_2$) were purchased from Chron Chemicals.

Synthesis of P(AA-co-Am) and P(AA-co-Am)/Ca^{2+}hydrogels

0.1 M of initiator (I2959) solution was prepared with ethanol. the different weights of VTESs (0 g, 30 mg, 60 mg, 90 mg) were added into 14 mL of at3.0 g of AA and 3.0 g of Am were dissolved in the VSNP solution and magnetically stirred for 30 minutes, followed by degassing to obtain precursor solutions. Finally, after adding initiator solution to the precursor solutions, the precursor solutions were poured into a polytetrafluoroethylene mould, and then irradiated under ultraviolet light (365 nm) for 60 minutes to obtain hydrogels. The as-prepared hydrogels were immersed in different concentrations of $CaCl_2$ solution (0.5 M, 1.0 M, 1.5 M, 2.0 M, 2.5 M) for 12 h to reach equilibrium, which was designated as P(AA-co-Am)/Ca^{2+}. The hydrogel prepared with and without the addition of VSNP was designated as P(AA-co-Am) and N-P(AA-co-Am), respectively.

Characterization

The attenuated total reflection Fourier-transform infrared spectroscopy of hydrogels was conducted using a spectrometer (Nicolet iS50, Thermo Fisher). Transmission-Electron Microscopy (TEM) electron microscope (Hitachi H7650, Hitachi, Japan) was used for transmission electron microscopy imaging of VSNPs at an accelerating voltage of: 100 kV. The TEM sample was obtained by fishing out the copper mesh after immersing in the VSNP solution. The samples underwent testing directly without any additional treatment. The internal microstructure for hydrogels was characterized using a scanning electron microscope (SEM) (Hitachi S4800, Hitachi, Japan). The hydrogel samples were quickly frozen with the help of liquid nitrogen and subsequently freeze-dried. The transparency of hydrogels was characterized using an ultraviolet and visible spectrophotometer (UV-Vis) in the range of 200-800 nm (UH4150, Hitachi, Japan). Rheological tests were performed on a Modular Compact Rheometer (MCR302, Anton Paar GMBH, Austria). The diameter of the rheometer flat probe is 25 mm. Disc-shaped hydrogel, with 27 mm diameter and 1 mm thickness, was fabricated and subsequently transferred to a parallel plate probe. In the course of shear strain scanning measurements, the strain was varied from 0.01 to 100% at angular frequency of 2 rad s^{-1}. In the course of angular frequency scanning measurements, the frequency was varied from 0.01 to 100 rad s^{-1} at a strain of 1%.

Self-healing, Self-adhesion and Biocompatibility Tests

The self-healing properties were evaluated after P(AA-co-Am) hydrogels healed for 5 h at room temperature without external stimuli. The self-adhesion properties were evaluated by using P(AA-co-Am) hydrogels to glue different substrates (skin, plastic, glass, and metal). The shear strength was measured with the lap shear testing method and acquired on a Universal Testing Machine with a separating speed of 100 mm min^{-1} (HY0580, Heng Yi, China). The biocompatibility of the P(AA-co-Am)/Ca^{2+} hydrogel was evaluated by placing a piece of hydrogel on the human skin for 12 h, and then removing it to observe for any allergic reactions.

Water Retention and Antifreeze Tests

The water retention ability of the P(AA-co-Am)/Ca^{2+} hydrogel tested by the weighing method with different time at humidity of 60% and 20°C. The weight ratio was defined as

$$\text{Weight ratio (\%)}=M_{\mathrm{i}} - M_0 \tag{1}$$

where M_{i} and M_0 represent the hydrogel mass at different times and the initial mass, respectively. The anti-freezing property of hydrogels was characterized on a Differential Thermal Scanner (DSC200F3, NETZSCH, Germany). A 10.0 mg sample, loaded in a hermetically sealed aluminium pan was cooled from 20^{o}C to -50^{o}C with a constant rate of 5^{o}C min^{-1} under constant nitrogen flow rate of 50 mL min^{-1}. Moreover, the antifreeze properties of hydrogels were evaluated through the photographs and conductivity tests at 20^{o}C and -20^{o}C.

Mechanical tests

Mechanical tests were performed on a Universal Tensile Testing Machine (HY0580, Heng Yi, China). Unless otherwise stated, a hydrogel sample with 20 × 6 × 1 mm (length × width × thickness) was used for the tensile testing at a temperature of 20°C and humidity of 60%, with a deformation rate of 50 mm min^{-1}. The loading-unloading curve was employed to evaluate the dissipative energy and hysteresis of the hydrogel. The dissipative energy (ΔE) was defined as the area enclosed by the loading-unloading process, calculated by the following formula:

$$\Delta E = (\int \sigma\, d\varepsilon)_{Loading} - (\int \sigma\, d\varepsilon)_{Unloading} \tag{2}$$

The hysteresis was defined by the Equation as the following formula:

$$Hysteresis = \Delta E / (\int \sigma\, d\varepsilon)_{Loading} \tag{3}$$

where σ and ε represent tensile stress and strain, respectively.

The tensile stress (σ) of hydrogels was defined by the Equation as the following formula:

$$\sigma = \frac{F}{A} \tag{4}$$

where F was the load force recorded by the universal machine and A was the cross-section area of hydrogels. The cross-section areas were calculated at as-prepared state and after immersing in the $CaCl_2$ solution for the P(AA-co-Am) hydrogel and the P(AA-co-Am)/Ca^{2+} hydrogel, respectively.

The tensile strain (ε) of the hydrogel microfiber was defined by the Equation as the following formula:

$$\varepsilon = \frac{l - l_0}{l_0} \times 100\% \tag{5}$$

where l_0 was the initial length of hydrogels between the fixtures and l was the length of hydrogels before breakage.

Electrical performance

The electrochemical workstation (CHI660E) was used to measure the electrochemical impedance spectroscopy of the hydrogel strain sensor, with a frequency range of 1 Hz to 1000 Hz and a voltage of 100 mV. Unless otherwise stated, the hydrogel strain sensor with 20 × 6 × 1 mm (length × width × thickness) was used for the electrical testing at a temperature of 20°C and humidity of 60%. The electrical resistance during the strain sensing was tested by connecting a nickel-plated copper sheet (6 mm x 7 mm rectangle) as an electrode to both ends of the hydrogel strain sensor to an LCR tester (IM3536). The LCR tester recorded the resistance signal of the hydrogel strain sensor during deformation, where the applied voltage was 1 V and the frequency was 800 Hz. The formula for calculating electrical conductivity (σ_e, S/m) was as follows:

$$\sigma_e = L/(R_0 * A) \tag{6}$$

Where L represented the length of the specimen, R_0 denoted the initial resistance, and A stranded for the cross-sectional area of the specimen. The relative resistance change ($\Delta R/R_0$) and Gauge factor (GF) were used to evaluate the sensing performance of the hydrogel strain sensor. The calculation formula was as follows:

$$\Delta R/R_0 = (R_s - R_0)/R_0 \tag{7}$$

$$GF = (\Delta R / R_0) / \varepsilon \quad (8)$$

where R_0 represented the original resistance before the application of strain, R_s represented the real-time resistance during the application of strain, and ε represented the strain.

Integration of the Sign Language Translation

The hydrogel, tinned copper sheet and copper wires was assembled to make a strain sensor (Fig. S16). Five hydrogel strain sensors were fixed to the second metacarpophalangeal joints of a right hand with medical adhesive tape. All the electronic components and the interconnecting conductive wires were connected on a 55 mm × 85 mm breadboard. The electric circuit diagram and the photograph of the printed circuit board were shown in Fig. S19. Program codes were written to the Arduino Nano board in advance to read signals from the analogue pins, which transmit signals and control the MP3 mini DFPlayer in real time. Fifteen recording files corresponding to the fifteen sign languages were stored in an SD card, which was then inserted in the card slot of the Audio player. A loudspeaker was connected to the MP3 mini DFPlayer.

All human body related experiments of wearable devices on a volunteer were performed in compliance with the relevant laws and institutional guidelines and under approval from Tiangong University. All participants were giving informed consent before participating in the study.

Supplementary Figures

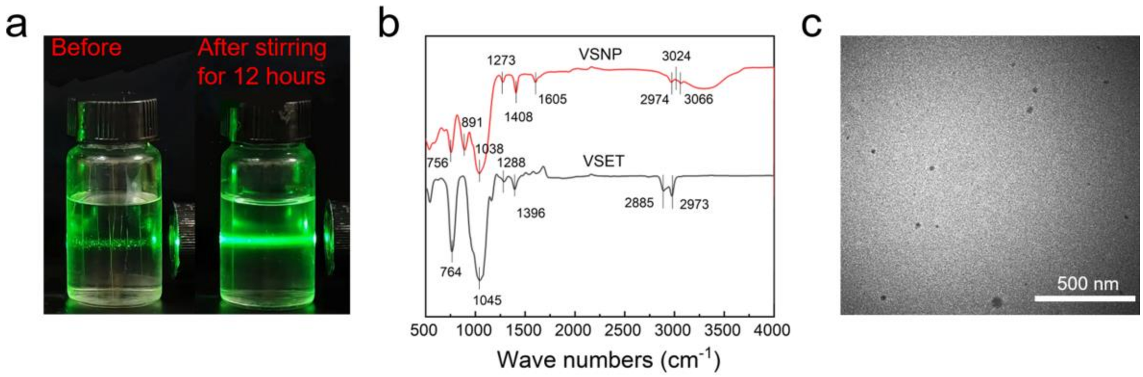

Fig. S1. Characterization of vinyl hybrid silica nanoparticles (VSNPs). (a) Photographs of the as-synthesized VSNPs: Before (left) and after (right) the sol-gel process. (b) Fourier transform infrared spectra of VTESs and VSNPs revealing vinyl groups dangling on the surface of VSNPs. (c) Transmission electron microscope image of highly monodispersed VSNPs with an average diameter of 16 nm.

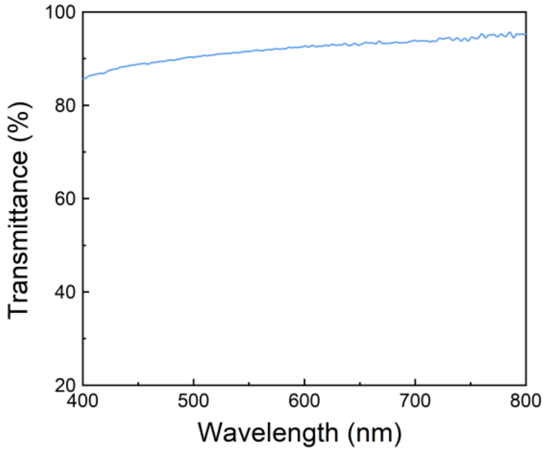

Fig. S2. Transmission spectra of the P(AA-co-Am)/Ca^{2+} hydrogel.

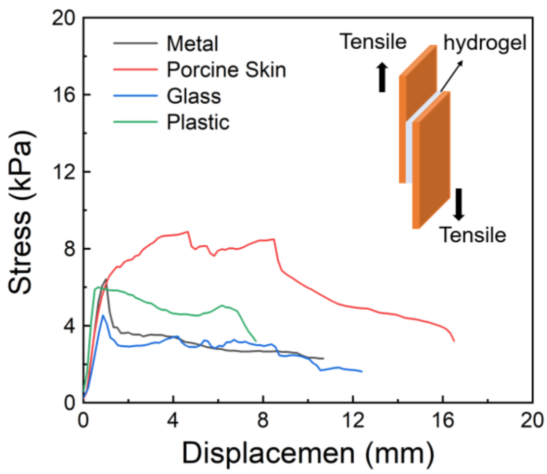

Fig. S3. Shear strengths of the P (AA-co-Am) hydrogel adhering to different substrates.

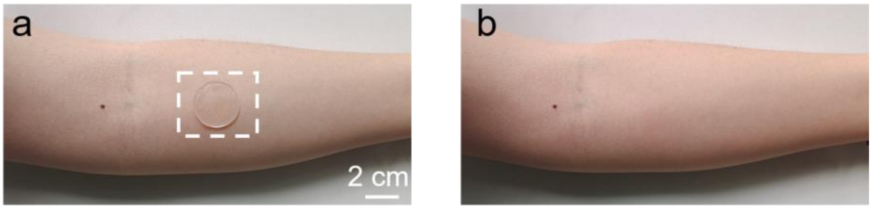

Fig. S4. The biocompatibility of the P(AA-co-Am)/Ca^{2+} hydrogel: (a) applied on human skin for 12 h, (b) skin condition after removal.

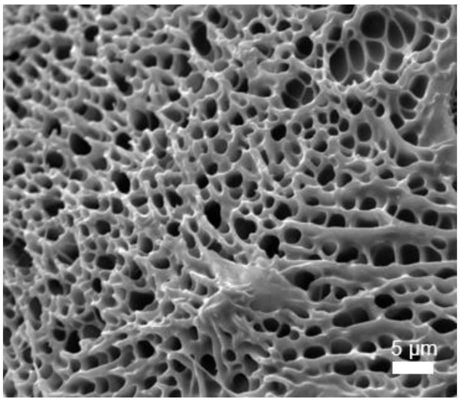

Fig. S5. The cross-section SEM image of the freeze-dried P(AA-co-Am)/Ca^{2+} hydrogel.

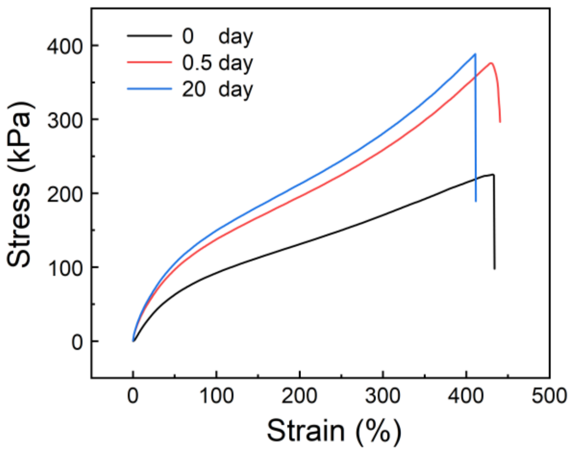

Fig. S6. Typical stress-strain curves of P(AA-co-Am)/Ca^{2+} hydrogels at a temperature of 20°C and humidity of 60% for different days.

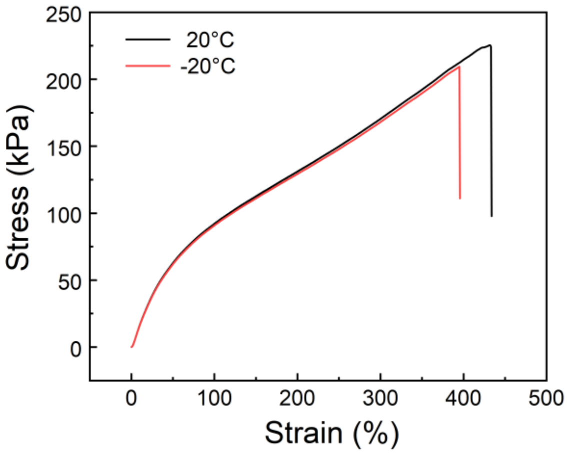

Fig. S7. Typical stress-strain curves of P(AA-co-Am)/Ca^{2+} hydrogels at different temperature.

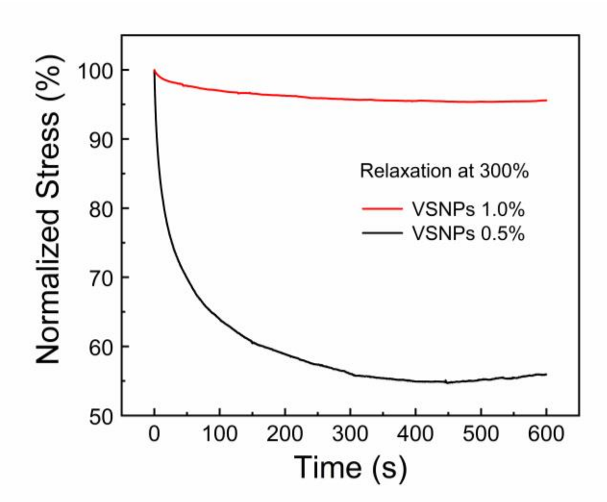

Fig. S8. Stress relaxation curves of P(AA-co-Am) hydrogels (at monomer mass of 30% and AA: Am of 1:1) with different VSNP contents.

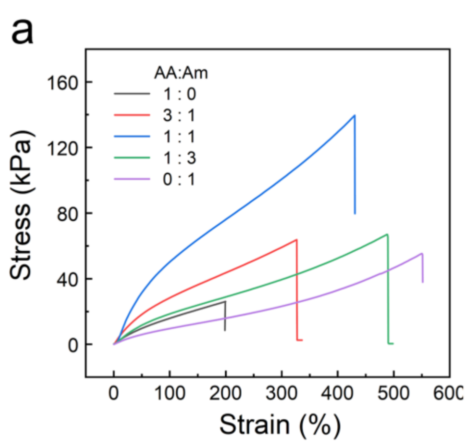

Fig. S9. (a) Typical stress-strain curves, (b) Stress-recovery curves of P(AA-co-Am) hydrogels (at monomer mass of 30% and VSNP contents of 1.0%) with different ratios of AA to Am.

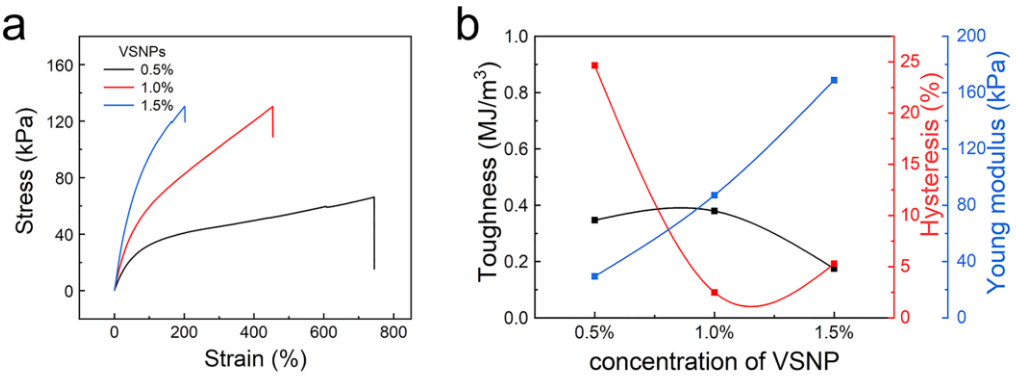

Fig. S10. (a) Typical stress-strain curves, (b) Toughness and Young's modulus and mechanical hysteresis of P(AA-co-Am) hydrogels (at monomer mass of 30% and AA: Am of 1:1) with different contents of VSNP.

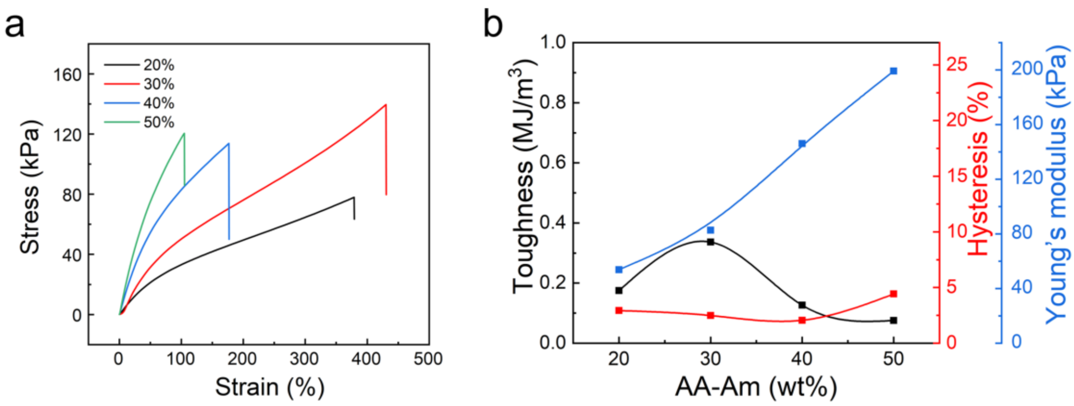

Fig. S11. (a) Typical stress-strain curves, (b) Toughness and Young's modulus and mechanical hysteresis of P(AA-co-Am) hydrogels (at VSNP contents of 1.0% and AA: Am of 1:1) with different contents of monomer mass.

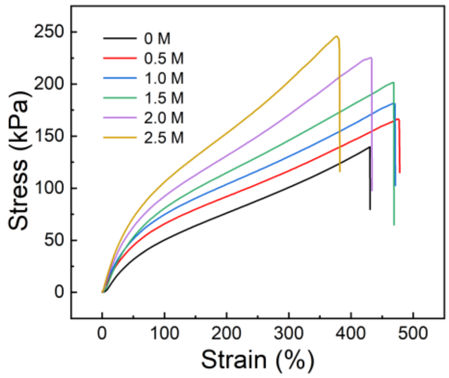

Fig. S12. Typical stress-strain curves of the P(AA-co-Am)/Ca^{2+} hydrogel (at VSNP contents of 1.0%, monomer mass of 30%, and AA: Am of 1:1) with different concentrations of $CaCl_2$.

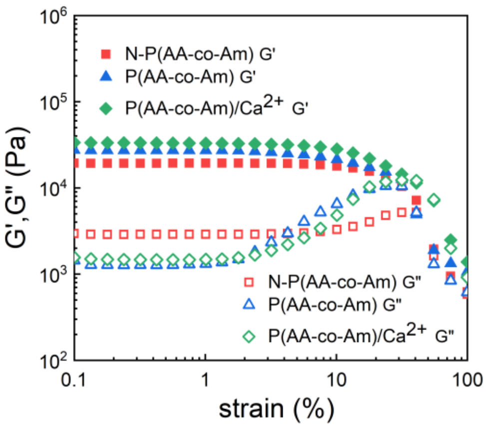

Fig. S13. Strain dependencies of the storage (G′) and loss (G″) moduli of hydrogels at angular frequency of 2 rad s^{-1}.

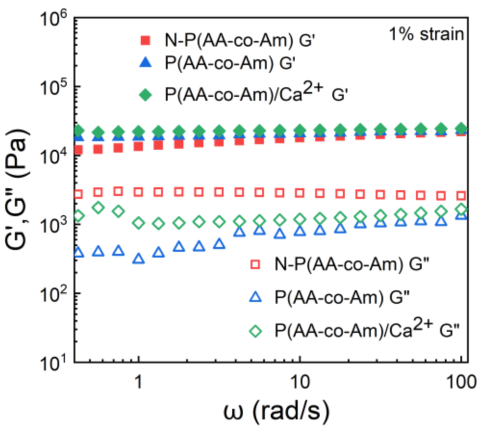

Fig. S14. Frequency dependencies of the storage (G′) and loss (G″) moduli of hydrogels at a strain of 1%.

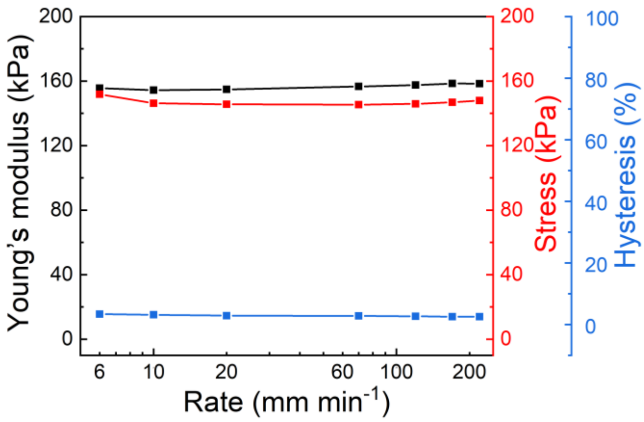

Fig. S15. Young's modulus, stress and hysteresis of P(AA-co-Am)/Ca^{2+} hydrogels at different strain rates.

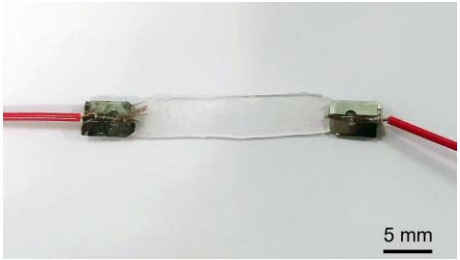

Fig. S16. Photograph of a strain sensor based on the hydrogel strain sensor.

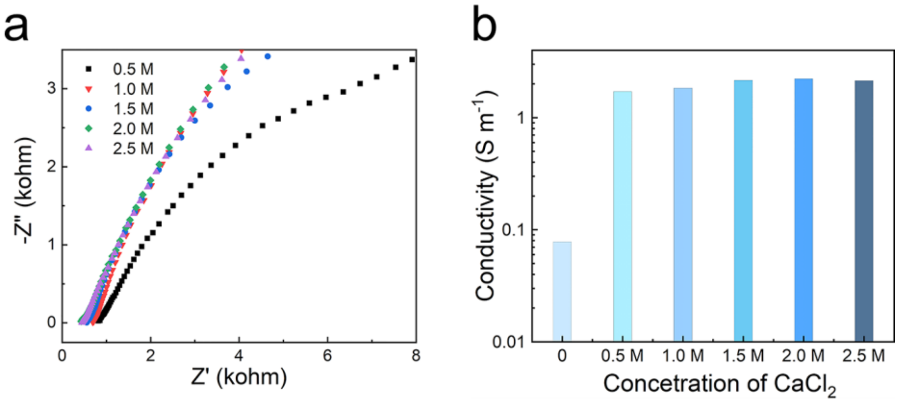

Fig. S17. (a) EIS Nyquist plots and (b) corresponding ionic conductivity of hydrogels with different concentrations of $CaCl_2$.

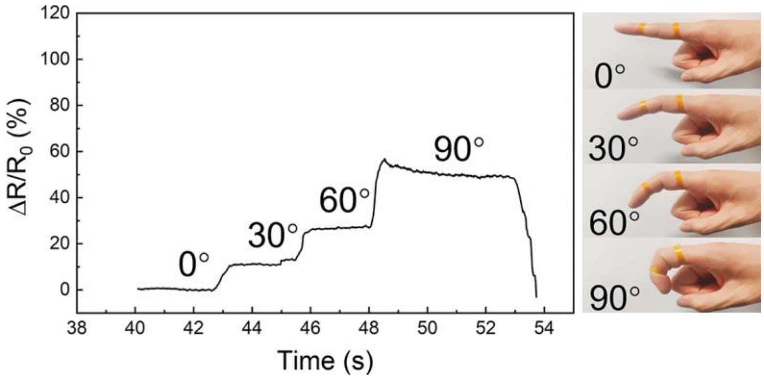

Fig. S18. Detection of knuckle flexion by the hydrogel strain sensor.

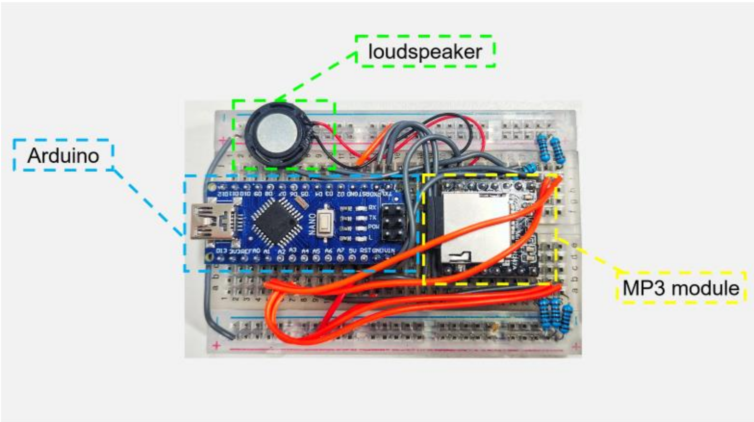

Fig. S19. The photograph of the printed circuit board.

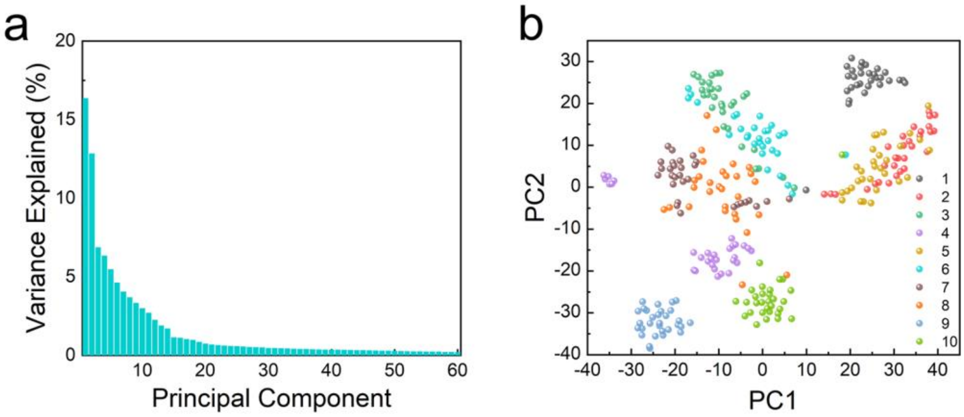

Fig. S20. (a) The variance contribution of the top 60 features of the 10 single gestures extracted by principal component analysis (PCA). (b) The scatter diagram of the training data of the 10 single gestures under the coordinate system composed of the first and the second principal component.

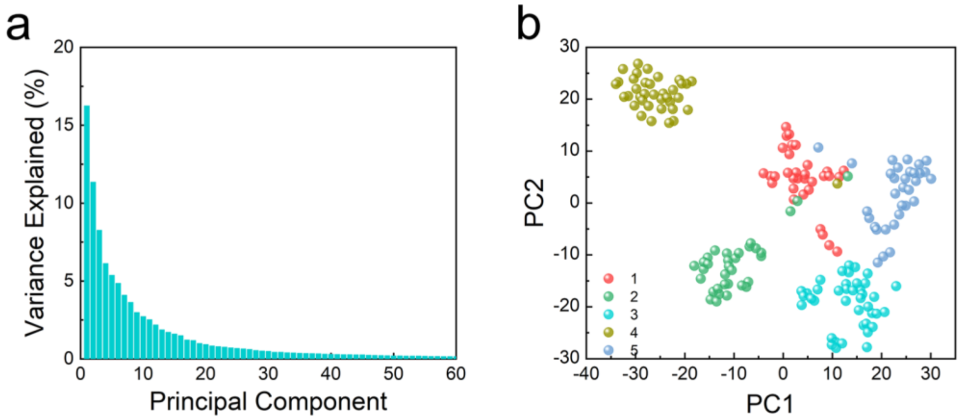

Fig. S21. (a) The variance contribution of the top 60 features of the 5 combined gestures extracted by principal component analysis (PCA). (b) The scatter diagram of the training data of the 5 combined gestures under the coordinate system composed of the first and the second principal component.

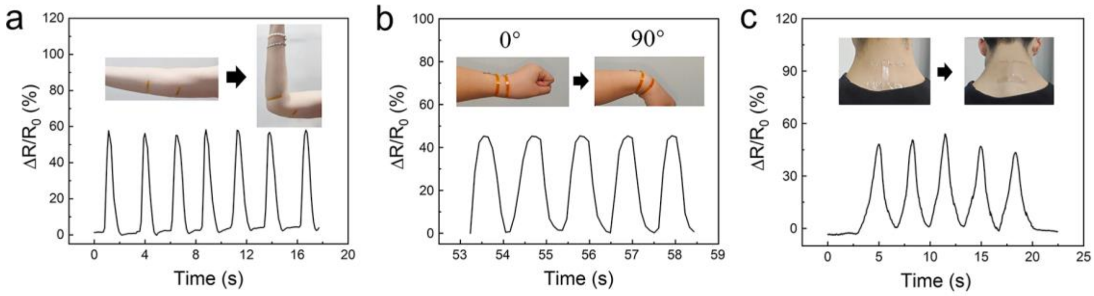

Fig. S22. Real-time monitoring of human movement by hydrogel strain sensor. a) Relative resistance changes of elbow flexion sensor. b) Relative resistance changes of wrist flexion sensor, c) Relative resistance changes of neck flexion sensor.

Supplementary Movie

Supplementary Movie S1. A demonstration of the control of the robotic arm by the sensor array.

Supplementary Movie S2. A demonstration of Gradient intelligent control of LED by hydrogel.

Supplementary Movie S3. A real-time translation demonstration of simple sign language.

Supplementary Movie S4. A real-time translation demonstration of complex sign language.